Superfluid properties of the inner crust of neutron stars

N. Sandulescu,[1,2,3] Nguyen Van Giai,[2] and R. J. Liotta[3]
[1]*Institute of Physics and Nuclear Engineering, 76900 Bucharest, Romania*
[2]*Institut de Physique Nucléaire, Université Paris-Sud, F-91406 Orsay Cedex, France*
[3]*Royal Institute of Technology, Alba Nova, SE-10691 Stockholm, Sweden*
(Received 11 February 2004; published 16 April 2004)

Superfluid properties of the inner crust matter of neutron stars, formed by nuclear clusters immersed in a dilute neutron gas, are analyzed in a self-consistent Hartree-Fock-Bogoliubov approach. The calculations are performed with two pairing forces, fixed so as to obtain in infinite nuclear matter the pairing gaps provided by the Gogny force or by induced interactions. It is shown that the nuclear clusters can either suppress or enhance the pairing correlations inside the inner crust matter, depending on the density of the surrounding neutrons. The profile of the pairing field in the inner crust is rather similar for both pairing forces, but the values of the pairing gaps are drastically reduced for the force which simulates the polarization effects in infinite neutron matter.

DOI: 10.1103/PhysRevC.69.045802 PACS number(s): 26.60.+c, 21.60.−n, 97.60.Jd

I. INTRODUCTION

The possibility of nuclear superfluidity in neutron stars was suggested long ago [1,2], before the first pulsars were actually observed. The first experimental fact pointing to the nuclear superfluidity in neutron stars was the large relaxation times which follow the sudden period changes (so-called "glitches") of pulsar rotation. Later on, the mechanism of the glitch phenomenon itself was directly related to the rotational behavior of the inner crust superfluid [3]. Thus, according to the present models the glitches are generated by a catastrophic unpinning of the superfluid vortex lines from the nuclei immersed in the inner crust of neutron stars.

Apart from the glitches phenomena, the superfluid properties of the inner crust matter have also important consequences on the cooling of neutron stars [4]. Thus, the heat diffusion from the interior of the star to the nuclear surface can be strongly suppressed in the crust region due to the energy gap in the excitation spectrum of the inner crust superfluid.

A fully microscopic calculation of pairing properties of inner crust matter should be based on a bare nucleon-nucleon force and should account for the polarization effects induced by the nuclear medium. However, this is a difficult problem which is not yet completely solved even for the pure neutron matter [5]. In addition to the uncertainty related to the appropriate pairing force, for the inner crust one has also to face the problem of calculating the pairing properties of a nonuniform nuclear system, in which the density is changing significantly from the center of the nuclear clusters to the dilute neutron matter in which the clusters are immersed.

The first calculations of the inner crust matter superfluidity were done by employing semiclassical pairing models based on a local density approximation [6]. Later on the calculations were performed also in the Hartree-Fock-Bogoliubov (HFB) approach [7]. In these works the mean field of the inner crust matter was fixed to a Woods-Saxon form and the pairing field was estimated by using a Gogny force [8] and a bare force (Argonne). The HFB calculations showed that the semiclassical pairing models overestimate the influence of the nuclear clusters on the pairing properties of the inner crust matter.

In this paper we present the pairing properties of the inner crust matter predicted by fully self-consistent HFB calculations in which both the mean field and the pairing field are calculated starting from effective two-body forces. In this way, the effects induced upon the pairing correlations by the strong local variations of the particle density and of the nucleon effective mass inside the inner crust matter are taken into account consistently. Moreover, the self-consistency allows us to study in more details how the properties of the nuclear clusters are affected by the external neutron gas in which they are embedded.

In the present HFB calculations the pairing correlations are evaluated by using a density-dependent contact force. The calculations are done with two sets of parameters, fixed to reproduce the superfluid properties of neutron matter given either by a Gogny force or by microscopic calculations which take into account polarization effects [9,10].

The paper is organized as follows. In Sec. II we present shortly the structure of the inner crust matter used in this study and we introduce the HFB approach. The results of the calculations are presented in Sec. III. In the first part of this section we analyze the density and the mean field distributions and in the second part we discuss the pairing properties. The summary and the conclusions are given in Sec. IV.

II. INNER CRUST MATTER AND THE HFB APPROACH

According to standard models the inner crust matter is formed by a lattice of neutron-rich nuclei immersed in a sea of unbound neutrons and relativistic electrons [11]. In the density range from neutron drip density ($\rho_d \approx 1.4\times10^{-3}\rho_0$, where $\rho_0 = 0.16$ fm^{-3} is the saturation density) to about half the saturation density, the nuclear clusters are most probably spherical and the unbound neutrons are in the $^1S_0$ superfluid phase. At higher densities, before the nuclear clusters are dissolved in the uniform matter of the core, other nonspheri-

cal nuclear configurations (e.g., rods, plates, tubes, bubbles) can be formed.

One of the first microscopic studies of the properties of inner crust matter was done in Ref. [12]. In this reference the distribution of the baryonic matter in the inner crust was evaluated by using a density functional suggested by the density matrix expansion method and adjusted on the neutron equation of state of Siemens-Pandharipande [13]. In these calculations the pairing correlations and the spin-orbit interaction for the neutrons were neglected. The calculations were performed in the Wigner-Seitz approximation, i.e., the inner crust matter is replaced by a set of noninteracting cells, each cell containing in its center a nuclear cluster surrounded by a gas of unbounded neutrons. In addition, in each Wigner-Seitz cell are uniformly distributed a number of relativistic electrons equal to the number of protons contained in the nuclear cluster.

In this study we analyze the superfluid properties of the inner crust matter starting from a set of such Wigner-Seitz cells determined in Ref [12]. More precisely, for a given total baryonic density and proton number we calculate in the HFB approach what are the mean fields and the pairing fields of the nuclear matter distributed in the Wigner-Seitz cells.

The HFB equations are solved here in the coordinate space. The calculations are performed by using a Skyrme-type force for the particle-hole channel and a zero-range pairing force in the particle-particle channel. In this case the HFB equations are local and for a spherically symmetric system they reduce to a set of radial equations [14,15]:

$$\begin{pmatrix} h(r)-\lambda & \Delta(r) \\ \Delta(r) & -h(r)+\lambda \end{pmatrix}\begin{pmatrix} U_i(r) \\ V_i(r) \end{pmatrix} = E_i \begin{pmatrix} U_i(r) \\ V_i(r) \end{pmatrix}, \tag{1}$$

where U_i, V_i are the upper and lower components of the radial HFB wave functions, λ is the chemical potential while $h(r)$ and $\Delta(r)$ are the mean field Hamiltonian and pairing field, respectively. They depend on particle density $\rho(r)$, abnormal pairing tensor $\kappa(r)$, kinetic energy density $\tau(r)$ and spin density $J(r)$ defined by

$$\rho(r) = \frac{1}{4\pi}\sum_i (2j_i+1)V_i^*(r)V_i(r), \tag{2}$$

$$\kappa(r) = \frac{1}{4\pi}\sum_i (2j_i+1)U_i^*(r)V_i(r), \tag{3}$$

$$J(r) = \frac{1}{4\pi}\sum_i (2j_i+1)\left[j_i(j_i+1) - l_i(l_i+1) - \frac{3}{4}\right]V_i^2, \tag{4}$$

$$\tau(r) = \frac{1}{4\pi}\sum_i (2j_i+1)\left[\left(\frac{dV_i}{dr} - \frac{V_i}{r}\right)^2 + \frac{l_i(l_i+1)}{r^2}V_i^2\right]. \tag{5}$$

The summations are over the whole positive-energy quasiparticle spectrum of the system. For the unbound quasiparticle states the summations should be replaced by integrals over the energy [16]. The general expressions of the mean field and pairing field on the densities are given in Ref. [15].

The HFB equations are applied here to the inhomogeneous matter of a spherical Wigner-Seitz cell, i.e., a nuclear cluster immersed in a sea of unbound neutrons. Thus, at relatively large distance from the nuclear cluster the particle density and the mean field should have constant nonzero values corresponding to a uniform neutron gas. In order to get this physical situation we impose at the cell radius R_c the following boundary conditions for the HFB solutions [12]: (i) even parity wave functions vanish at $r=R_c$; (ii) first derivatives of odd-parity wave functions vanish at $r=R_c$. With these mixed boundary conditions at the cell border the continuous quasiparticle spectrum is discretized and all the HFB wave functions corresponding to bound and unbound states are normalized in the Wigner-Seitz cell.

In the HFB calculations we use for the particle-hole channel the Skyrme effective interaction SLy4 [17]. This interaction has been adjusted to describe properly nuclei with a large neutron excess as well as the properties of neutron matter. Due to these constraints one expects that the nuclear matter distribution provided by SLy4 is not far from the one estimated in Ref. [12]. Thus, as seen from the calculations presented in Ref. [18] the force SLy4 predicts for the inner crust matter almost the same maximum density and proton fractions as the density functional employed in Ref. [12].

The pairing field is calculated here with a density-dependent contact force of the following form [19]:

$$V(\mathbf{r}-\mathbf{r}') = V_0\left[1 - \eta\left(\frac{\rho}{\rho_0}\right)^\alpha\right]\delta(\mathbf{r}-\mathbf{r}') \equiv V_{eff}(\rho(r))\,\delta(\mathbf{r}-\mathbf{r}'). \tag{6}$$

With this force the pairing field is local and is given by

$$\Delta(r) = V_{eff}(\rho(r))\,\kappa(r). \tag{7}$$

Since the pairing force has a zero range the HFB calculations should be performed with an energy cutoff for the quasiparticle spectrum.

For the parameters of the pairing force we use the following values: $V_0=-430.0$ MeV fm^3, $\eta=0.7$, and $\alpha=0.45$. With these values and with a cutoff energy equal to 60 MeV we reproduce approximately the pairing properties of neutron matter given by the Gogny force [19,20]. In Sec. III B we perform also a HFB calculation with a second set of parameters for the pairing force adjusted to reproduce the gap values of neutron matter predicted by calculations which take into account in-medium polarization effects.

III. HFB PROPERTIES OF INNER CRUST MATTER

As we have mentioned in the preceding section, the HFB calculations will be performed for a set of representative Wigner-Seitz cells determined in Ref. [12].

The maximum density for the inner crust considered in Ref. [12] is $\rho_{max}=0.0789$ fm^{-3} and corresponds to a cell formed by 32 protons and 950 neutrons. Above this density the energy per baryon becomes close to the value of the uniform neutron system and other nonspherical configurations might be formed. The density region between the neutron drip density ρ_d and ρ_{max} is divided in Ref. [12] into 11

domains. What is remarkable is that the cells corresponding to densities smaller than ρ_{max} contain only 50 or 40 protons.

From all the cells with 50 protons we will consider here only two representative cells, i.e., one with the density $\rho = 0.0204$ fm^{-3} and containing 1750 neutrons, and one with the density $\rho = 0.003\,73$ fm^{-3} and having 900 neutrons. These cells have the maximum and the minimum densities for 50 protons. Following Ref. [12] we denote the cells like a nucleus with Z protons and N neutrons. Thus, the two cells with $Z=50$ will be denoted by ^{1800}Sn and ^{950}Sn.

We consider also two representative cells with $Z=40$ protons, namely ^{1500}Zr and ^{500}Zr. These cells correspond to the densities $\rho = 0.0475$ fm^{-3} and $\rho = 0.001\,59$ fm^{-3}, respectively. The cell ^{1500}Zr is the highest density cell with $Z=40$ while the cell ^{500}Zr corresponds to the lowest positive binding energy per nucleon.

For the four cells chosen above we present first the predictions of the HFB calculations for the densities and the mean fields of the nuclear clusters and the surrounding neutron gas. Then, we analyze how the distortions of the density distributions induced by the clusters affect the pairing properties of nuclear matter inside the cells.

A. Density and mean field distributions

In finite nuclei there is always a maximum number of neutrons which can be bound for a given number of protons. This neutron stability limit, which defines the neutron dripline, has been extensively studied theoretically in the recent years. Experimentally there are drastic limitations for approaching the neutron dripline in the laboratory since the neutron-rich nuclei are quickly β decaying. This is not the case for the neutron-rich nuclei immersed in the inner crust since here the β decay is blocked by the presence of the degenerate electron gas uniformly distributed throughout the baryonic matter. Consequently, inside the inner crust the nuclei can bind more neutrons than the nuclei in the vacuum. In addition, their density and mean field can change significantly due to the presence of the surrounding neutron gas.

These changes will be analyzed first for the case of the Wigner-Seitz cells having 50 protons. The HFB calculations with the SLy4 force and the pairing interaction mentioned in Sec. II predict for the isolated Sn isotopes the dripline for two-neutron separation at $N=126$. Adding two more neutrons to ^{176}Sn the nuclear system in the vacuum is losing about 1 MeV from its binding.

In Figs. 1 and 2 the densities and mean fields of the dripline nucleus ^{176}Sn are compared to the corresponding quantities of the nuclear cluster immersed in the neutron gas. For the cell ^{950}Sn one can see that the nuclear cluster and the dripline nucleus ^{176}Sn have similar properties. Moreover, the number of bound neutrons inside the cluster is also equal to $N=126$. The situation is rather different for the cell ^{1800}Sn where the density of the outer neutron gas is much higher. Thus, it can be seen that the neutron density and the neutron mean field profiles have an extended "surface" before they reach the constant values corresponding to the neutron gas. In spite of these significant modifications of the density and the mean field, the number of bound neutrons inside the cluster, i.e., the neutrons with single-particle energies below the constant value of the mean field corresponding to the neutron gas, is still equal to $N=126$. On the other hand, if one integrates the neutron density up to $r=12$ fm, where approximatively the density profile is becoming constant, one finds about 300 neutrons. Thus, it appears that the large surface is generated in fact by the unbound neutrons which are partially localized in the cluster region due to the interaction with the bound nucleons.

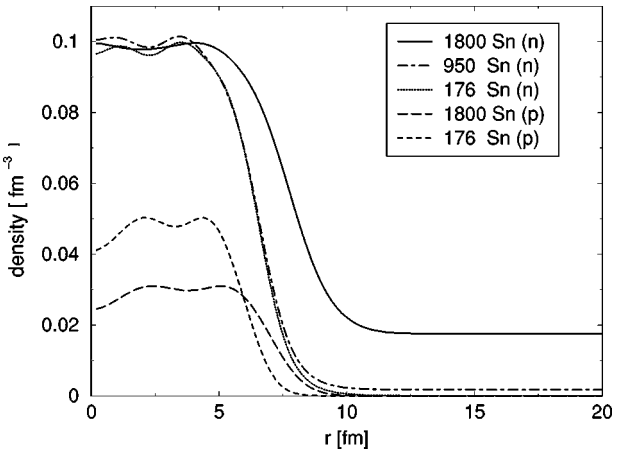

FIG. 1. Neutron and proton densities for the Wigner-Seitz cells with 50 protons and for the dripline nucleus ^{176}Sn. The cells to which the neutron densities (n) and proton densities (p) correspond are denoted by the total number of nucleons in the cell.

Next, we discuss the properties of the nuclear clusters with 40 protons. The neutron dripline for isolated Zr isotopes is located at $N=82$. However, in this case the two-neutron separation energy curve is crossing zero with a very small slope. Compared to ^{122}Zr the binding energy of ^{124}Zr is only about 200 keV smaller. This is due to the proximity of the resonant states $3f_{7/2}$ and $3p_{3/2}$ to the continuum threshold and the fact that these states can easily accommodate more neutrons without losing too much binding energy [21]. Thus, one expects that by immersing the dripline nucleus ^{122}Zr in

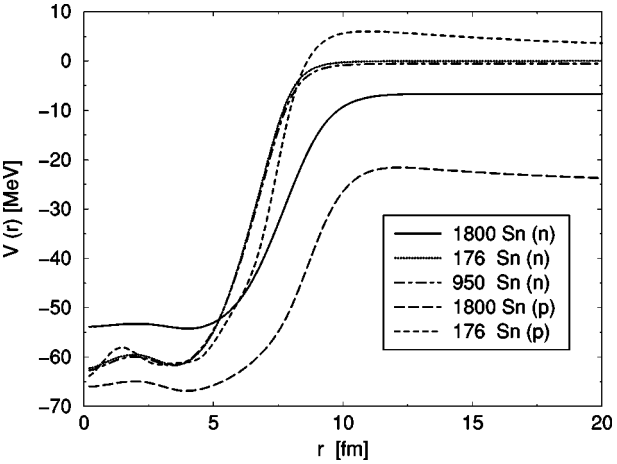

FIG. 2. The mean fields for the Wigner-Seitz cells with 50 protons and for the dripline nucleus ^{176}Sn. The notations are the same as in Fig. 1.

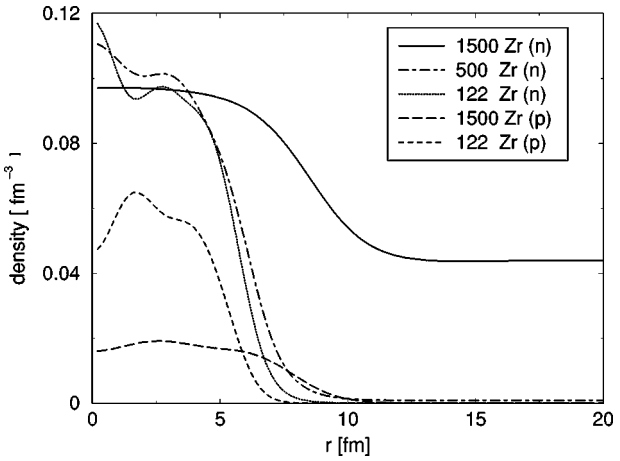

FIG. 3. Neutron and proton densities for the Wigner-Seitz cells with 40 protons and for the dripline nucleus ^{122}Zr. The notations are the same as in Fig. 1.

the neutron gas one can easily gain the small extra energy necessary to bind more neutrons in the cluster. This is actually the case even for the low-density cell ^{500}Zr. The density and the mean field profiles for this cell are shown in Figs. 3 and 4. From Fig. 3 one can see that although the density of the outer neutrons is about half compared to the cell ^{900}Sn, they change more significantly the density profile of the dripline nucleus ^{122}Zr than for ^{176}Sn. Due to these changes the resonant states $3f_{7/2}$ and $3p_{3/2}$ become bound, increasing by 12 the number of bound neutrons inside the nuclear cluster.

By increasing the density of the outer neutron gas one expects further changes of the nuclear cluster formed around 40 protons. These changes can be seen in Figs. 3 and 4 for the cell ^{1500}Zr. However, although the density of the outer neutron gas is now more than 20 times greater than in the cell ^{500}Zr, the number of bound neutrons in the cluster is increasing only by about ten neutrons. The total number of neutrons found by integrating the density up to $r=12$ fm is about 300 neutrons, as in the cell ^{1800}Sn.

In conclusion we find that the nuclear clusters immersed in the neutron gas keep many features of the dripline nucleus

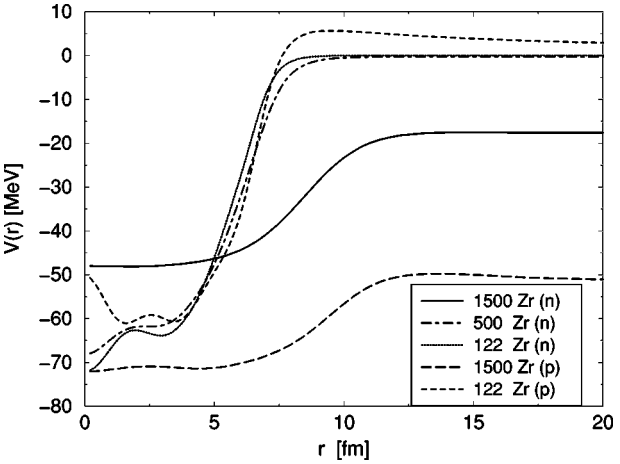

FIG. 4. The mean fields for the Wigner-Seitz cells with 40 protons and for the dripline nucleus ^{122}Zr. The notations are the same as in Fig. 1.

having the same number of protons. For the cells with large neutron densities one finds a thick surfacelike structure which is developing in the transition region from the center of the cell to the neutron gas regime. This surface structure is mainly formed by unbound neutrons which are partially kept localized in the surface region by the interaction with the nucleons bound inside the nuclear cluster.

B. Superfluid properties

As we have seen in the preceding subsection, the density of the neutron matter is changing significantly from the center of the cell, where the nuclear cluster is located, to its edge filled by the uniform neutron gas. As shown by all the microscopic calculations, the pairing gap of the neutron matter depends strongly on the density. The majority of the calculations predict that as function of density the pairing gap has a bell shape form, with the maximum at a density equal to about one-fifth the saturation density [5]. However, what is the maximum value of the gap and its detailed density dependence are still subjects of debate. Thus, the BCS-type calculations based on bare forces give a maximum gap of about 3 MeV and no pairing for nuclear matter at saturation density. Almost the same maximum gap one gets with a Gogny force, but the gap falls to a finite value of about 1 MeV at the saturation density. On the other hand, all the microscopic calculations which go beyond the BCS approximation show that the gap is strongly reduced by the screening and self-energy effects. However, the amount of the gap suppression and even the density dependence of the gap depend on the employed approximations. The most recent calculations point to a maximum gap of about 1 MeV [9,10,22]. How this value of the pairing gap could be reconciled with the pairing gap in finite nuclei is still an open question.

Since at present it is not yet established what are the pairing properties of neutron matter, we perform here two calculations for the inner crust matter. In one calculation we fix the density-dependent δ force such as to reproduce approximately the gap values of neutron matter provided by the Gogny force. The parameters of this pairing force, which we have used above for analyzing the density and the mean field properties of the inner crust matter, are given at the end of Sec. II. In the second calculation, we fix the parameters of the pairing force so as to obtain for neutron matter a maximum gap of about 1 MeV, as in the microscopic calculations which take into account the screening and the self-energy effects [9,10]. Since in this case the shape of the density dependence is unclear, we preferred to change only the strength of the force, which was reduced to the value $V_0=-330$ MeV fm^{-3}, and to keep the other two parameters as in the previous calculations. For the cutoff energy we used in both calculations the same value, i.e., $E_c=60$ MeV.

First, we discuss the results given by the pairing interaction fitted to the Gogny force. The pairing fields calculated for the two cells with 50 protons are shown in Fig. 5. For the cell ^{1800}Sn one can see that the pairing field is about two times smaller (here and below we refer to the absolute values of the pairing field) in the center of the cell compared to the value in the region of the uniform neutron gas. We can also

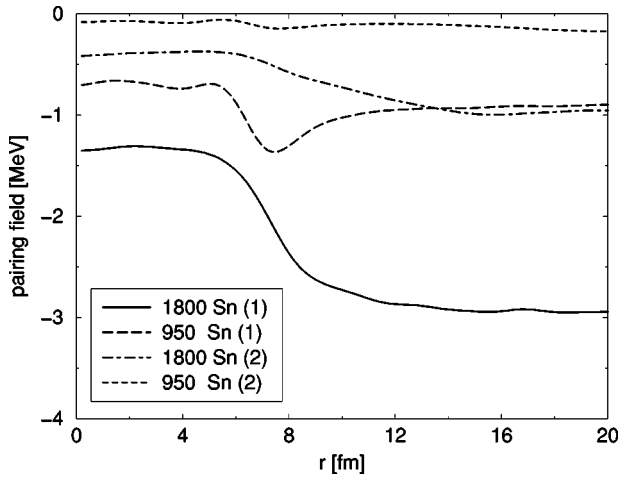

FIG. 5. The neutron pairing fields for the Wigner-Seitz cells with 50 protons. The full and the long-dashed lines correspond to the pairing fields calculated with the first pairing force while the dashed-dotted and the dashed lines correspond to the second pairing force.

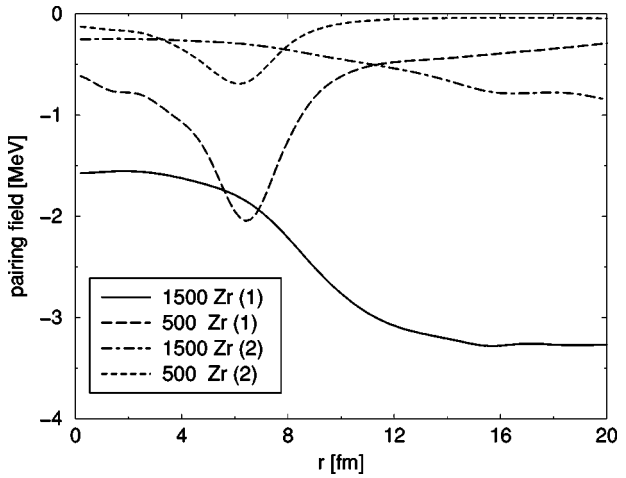

FIG. 6. The neutron pairing fields for the Wigner-Seitz cells with 40 protons. The full and the long-dashed lines correspond to the pairing fields calculated with the first pairing force while the dashed-dotted and the dashed lines correspond to the second pairing force.

see that the pairing field is decreasing continuously towards the center of the cell.

This is not the case for the cell ^{950}Sn. For this cell we observe that in passing from the low density region of the neutron gas towards the high-density region of the cluster, the pairing field is increasing in the intermediate density region of the cluster surface. This is a manifestation of the bell shape dependence of the pairing gap on density. Thus, for the cell ^{950}Sn the density of the outer neutron gas is much smaller than the value for which the gap is maximum, which is reached in the surface region. In the case of the cell ^{1800}Sn the density for which the gap is maximum is already reached in the neutron gas region.

The behavior of the pairing field in the cells with 40 protons is rather similar with that found in the two cells discussed above. As seen in Fig. 6, for the cell ^{500}Zr we observe also an increase of the gap in the surface region, which is now more pronounced than for the cell ^{950}Sn. One can also notice that this significant increase of the pairing field in the surface region is extending rather deeply towards the center of the cell. Consequently, the pairing field inside the nuclear cluster region is not becoming anymore smaller than in the neutron gas region.

In all the cells we observe that the slope of the pairing field is changing very slowly when it is crossing the region between the nuclear cluster and the uniform neutron gas. This behavior, sometimes referred to as the proximity effect [7], is related to the large size of Cooper pairs in low-density nuclear matter. The large diffusivity of the pairing field in the surface region, which is also seen in finite nuclei, is accentuated here by the fact that the superfluidity in the surface is carried mainly by the unbound neutrons, which are only partially localized at the interface between the nuclear cluster and the neutron gas.

Next, we discuss the results corresponding to the second pairing force which simulates the polarization effects. The pairing fields obtained with this pairing force are shown in Figs. 5 and 6 by short-dashed and dashed-dotted lines. As expected, the pairing correlations are reduced strongly for all the cells. For the high-density cells ^{1800}Sn and ^{1500}Zr we can see that, in spite of the drastic suppression of the gap values, the profiles of the pairing fields are not changing very much compared to the previous calculations. For the low-density cell ^{950}Sn we can see that the pairing field is becoming very small almost everywhere in the cell. However, in the cell ^{500}Zr the pairing field is still showing a significant increase in the cluster surface and it is almost vanishing in the neutron gas region.

Thus, the behavior of the pairing field in the inner crust matter is rather complex. As we have seen above, the nuclear clusters not only can suppress but also enhance the pairing field inside the inner crust matter. On the other hand, the magnitude of the pairing field inside the inner crust depends very strongly on the scenario used for the pairing properties of infinite neutron matter.

IV. SUMMARY AND CONCLUSIONS

In this paper we have analyzed the properties of the inner crust matter in a self-consistent HFB approach. In the calculations we used for the particle-hole force a Skyrme-type interaction, i.e., SLy4, which is able to describe properly the basic properties of finite nuclei and infinite neutron matter. As pairing interaction we have chosen a density-dependent contact force. The parameters of the force were fixed so as to obtain for infinite neutron matter the pairing properties predicted by two calculations, i.e., a BCS calculation based on Gogny force and a microscopic calculation based on induced interactions.

The HFB calculations were performed for a set of Wigner-Seitz cells representative of the structure of the inner crust matter. First we have studied the density and the mean field distributions inside the cells and we have analyzed the properties of the nuclear clusters formed in the center of the

cells. Then, we have studied how the pairing field is modified inside the cells by the presence of the nuclear clusters. We have thus found that, for the cells corresponding to high baryonic densities, the pairing field is generally suppressed in the region of the nuclear cluster. This is not the case for the low-density cells where the pairing field is increasing significantly in the surface region of the cluster compared to the region of the uniform neutron gas.

The behavior of the pairing field inside the cells is rather similar for both pairing forces. However, the values of the pairing gaps are suppressed dramatically if the pairing force which simulates the polarization effects is used in the HFB calculations.

The complex behavior of the pairing field discussed here has important consequences on the thermal properties of the inner crust matter. These aspects are analyzed in a separate paper [23].

ACKNOWLEDGMENTS

N.S. acknowledges IPN-Orsay, KTH-Stockholm and the Swedish Programme for Cooperation in Research and Higher Education (STINT) for financial support.

[1] A. B. Migdal, Nucl. Phys. **13**, 655 (1959).
[2] V. L. Ginzburg and D. A. Kirzhnits, Zh. Eksp. Teor. Fiz. **47**, 2006 (1964) [Sov. Phys. JETP **20**, 1346 (1964)].
[3] P. W. Anderson and N. Itoh, Nature (London) **256**, 25 (1975).
[4] J. M. Lattimer, K. A. Van Riper, M. Prakash, and M. Prakash, Astrophys. J. **425**, 802 (1994).
[5] U. Lombardo, in *Nuclear Methods and the Nuclear Equation of State*, edited by M. Baldo (World Scientific, Singapore, 1999), pp. 458–510.
[6] R. A. Broglia, F. De Blasio, G. Lazzari, M. Lazzari, and P. M. Pizzochero, Phys. Rev. D **50**, 4781 (1994); F. De Blasio *et al.*, *ibid.* **53**, 4226 (1996).
[7] F. Barranco, R. A. Broglia, H. Esbensen, and E. Vigezzi, Phys. Rev. C **58**, 1257 (1998); F. Barranco *et al.*, Phys. Lett. B **390**, 13 (1997).
[8] J. Dechargé and D. Gogny, Phys. Rev. C **21**, 1568 (1980).
[9] J. Wambach, T. L. Ainsworth, and D. Pines, Nucl. Phys. **A555**, 128 (1993).
[10] C. Shen, U. Lombardo, P. Schuck, W. Zuo, and N. Sandulescu, Phys. Rev. C **67**, 061302(R) (2003).
[11] C. J. Pethick and D. G. Ravenhall, Annu. Rev. Nucl. Part. Sci. **45**, 429 (1995).
[12] J. W. Negele and D. Vautherin, Nucl. Phys. **A207**, 298 (1973).
[13] P. J. Siemens and V. R. Pandharipande, Nucl. Phys. **A173**, 561 (1971).
[14] A. Bulgac, Institute of Atomic Physics Report No. FT-194-1980, 1980; nucl-th/9907088
[15] J. Dobaczewski, H. Flocard, and J. Treiner, Nucl. Phys. **A422**, 103 (1984).
[16] M. Grasso, N. Sandulescu, Nguyen Van Giai, and R. J. Liotta, Phys. Rev. C **64**, 064321 (2001).
[17] E. Chabanat, P. Bonche, P. Haensel, J. Meyer, and R. Schaeffer, Nucl. Phys. **A627**, 710 (1997); E. Chabanat *et al.*, *ibid.* **A635**, 231 (1998).
[18] F. Douchin and P. Haensel, Phys. Lett. B **485**, 107 (2000).
[19] G. F. Bertsch and H. Esbensen, Ann. Phys. (N.Y.) **209**, 327 (1991).
[20] E. Garrido, P. Sarriguren, E. Moya de Guerra, and P. Schuck, Phys. Rev. C **60**, 064312 (1999).
[21] N. Sandulescu, L. S. Geng, H. Toki, and G. Hillhouse, Phys. Rev. C **68**, 054323 (2003).
[22] Achim Schwenk, Bengt Friman, and Gerald E. Brown, Nucl. Phys. **A713**, 191 (2003).
[23] N. Sandulescu, nucl-th/0403019.